Observed climate change hotspots

AGU PUBLICATIONS

Geophysical Research Letters

RESEARCH LETTER
10.1002/2015GL063891

Key Points:
- We determine climatic hotspots based on observations
- Observed hotspots are remarkably consistent with those from future projections
- Climate variability has not changed substantially during the period 1951–2010

Supporting Information:
- Text S1–S4, Figures S1–S9, and Tables S1–S6
- Text S1–S4
- Figure S1
- Figure S2
- Figure S3
- Figure S4
- Figure S5
- Figure S6
- Figure S7
- Figure S8
- Figure S9

Correspondence to:
M. Turco,
m.turco@isac.cnr.it

Citation:
Turco, M., E. Palazzi, J. von Hardenberg, and A. Provenzale (2015), Observed climate change hotspots, *Geophys. Res. Lett.*, *42*, 3521–3528, doi:10.1002/2015GL063891.

Received 17 MAR 2015
Accepted 4 APR 2015
Accepted article online 9 APR 2015
Published online 12 MAY 2015

Observed climate change hotspots

M. Turco[1], E. Palazzi[1], J. von Hardenberg[1], and A. Provenzale[2]

[1]Institute of Atmospheric Sciences and Climate, National Research Council, Torino, Italy, [2]Institute of Geosciences and Earth Resources, National Research Council, Pisa, Italy

Abstract We quantify climate change hotspots from observations, taking into account the differences in precipitation and temperature statistics (mean, variability, and extremes) between 1981–2010 and 1951–1980. Areas in the Amazon, the Sahel, tropical West Africa, Indonesia, and central eastern Asia emerge as primary observed hotspots. The main contributing factors are the global increase in mean temperatures, the intensification of extreme hot-season occurrence in low-latitude regions and the decrease of precipitation over central Africa. Temperature and precipitation variability have been substantially stable over the past decades, with only a few areas showing significant changes against the background climate variability. The regions identified from the observations are remarkably similar to those defined from projections of global climate models under a "business-as-usual" scenario, indicating that climate change hotspots are robust and persistent over time. These results provide a useful background to develop global policy decisions on adaptation and mitigation priorities over near-time horizons.

1. Introduction

Identifying the geographical regions where the climate is changing most is a topic of central interest in Earth System research (see, e.g., the last Intergovernmental Panel on Climate Change (IPCC) report [*Stocker et al.*, 2013]). Although the impacts of climate change are determined also by the vulnerability, finding where climate changes are larger is a crucial step in risk assessment and adaptation strategies. Climate change hotspots have been defined as regions which display the largest variations in multiple statistics (mean, variability, and extremes) of climate variables [*Giorgi*, 2006; *de Sherbinin*, 2014]. Previous studies have analyzed climate model projections to identify future hotspots [*Baettig et al.*, 2007; *Diffenbaugh et al.*, 2007; *Williams et al.*, 2007; *Loarie et al.*, 2009; *Beaumont et al.*, 2011; *Diffenbaugh and Giorgi*, 2012; *Diffenbaugh and Field*, 2013; *Piontek et al.*, 2014].

But what are the *observed* climate change hotspots? Most studies relying on observations at global scale have examined variations in the means. The analysis results generally indicate robust changes in mean temperatures, with significantly increasing values and large regional variations [*Karoly and Braganza*, 2001; *Hansen et al.*, 2010; *Jones et al.*, 2012; *Muller et al.*, 2013], and in mean precipitation, with positive trends over midlatitude land areas in the Northern Hemisphere and negative trends in central Africa [*Polson et al.*, 2013; *Stocker et al.*, 2013]. Instead, concurrent changes in observed precipitation and temperature statistics have been analyzed more seldom [*Hansen et al.*, 1998; *Hao et al.*, 2013; *AghaKouchak et al.*, 2014] and also variations in statistics different from the mean (e.g., variability) have received less attention, despite their impact on societies and ecosystems [see, e.g., *Schär et al.*, 2004; *Holmgren et al.*, 2013]. For instance, it is yet under debate how temperature variability has changed in the recent past [*Hansen et al.*, 2012; *Huntingford et al.*, 2013], while only a few studies have analyzed changes in precipitation variability [*Tsonis*, 1996; *Sun et al.*, 2012]. Common key concerns for these assessments are limitations in the spatial and temporal coverage and homogeneity of the data [*Wan et al.*, 2013]. For instance, some studies have detected an intensification of indices of extremes based on daily observational data sets [*Kiktev et al.*, 2003; *Donat and Alexander*, 2012; *Fischer and Knutti*, 2014], but these data are available only over a limited portion of the land fraction with higher coverage over northern midlatitudes [*Donat et al.*, 2013].

Global monthly data sets that allow a more global assessment and cover the last 60 years are now available. In this study we characterize the observed climate changes in the mean, variability, and extremes of seasonal temperatures and precipitation, identifying the observed climate change hotspots and providing relevant information on the most responsive areas. Our aim is to focus on robust observed changes that are easy to

communicate and can be used by policy and decision makers. To this end, we use the last available versions of state-of-the-art, well-established gridded databases.

2. Hotspot Identification

To quantify observed climate change hotspot index we follow the same approach of the study by *Diffenbaugh and Giorgi* [2012]. They quantified climate change in the models participating in the Climate Model Intercomparison Project phase 5, aggregating changes in the mean and variability of seasonal temperature and precipitation, and including information on seasons exceeding baseline extremes. Mathematically, the hotspot index is defined as the Standard Euclidean Distance:

$$\mathrm{SED}_{\mathrm{tot}} = \sqrt{\sum_{i}^{N_{\mathrm{indicators}}} \sum_{j}^{4} \left(\frac{\Delta_{ij}}{p_{95}(|\Delta_{ij}|)} \right)^2}, \tag{1}$$

where Δ_{ij} is the ith change indicator in the jth season at each grid point, as discussed below, and $p_{95}(|\Delta_{ij}|)$ is the 95th percentile of the global distribution of absolute values of the ith change indicator in the jth season.

The indicators Δ_{ij} are computed separately for each season (December-January-February (DJF), March-April-May (MAM), June-July-August (JJA), and September-October-November (SON)), and the changes refer to the differences between two consecutive periods, present: 1981–2010 and past: 1951–1980. Each period spans three decades, that is, the classical length of time to calculate climatic "normals" as defined by the World Meteorological Organization [*Bye et al.*, 2011]. The metric employed considers seven climate change indicators, namely, (1) absolute change in mean temperature, ΔT; (2) percentual change in mean precipitation with respect to the mean over 1951–1980, ΔP; (3) percentual change in the interannual standard deviation of the detrended temperature, ΔT_{var}; (4) percentual change in the interannual coefficient of variation of the detrended precipitation, ΔP_{var}; (5) frequency of seasons with temperatures exceeding the temperature maximum in the 1951–1980 period, f_{hot}; (6) frequency of seasons with precipitation exceeding the precipitation maximum in 1951–1980, f_{wet}; and (7) frequency of seasons with precipitation below the minimum seasonal precipitation in 1951–1980, f_{dry}.

A resampling method is used to assess the statistical significance of the observed differences at each grid point. To test the results against the null hypothesis of no change, for each time series we create 1000 surrogate time series by randomly shuffling (without repetition) the original signal, thus generating an ensemble of records where the possible temporal changes have been shuffled out. This provides 1000 surrogate values of the differences between the two subperiods, which are used to estimate the confidence intervals for no change at each grid point. We use the same shuffling sequence for all grid points within each iteration. More details on this test are provided in the supporting information.

3. Observational Data

We use global observations from several monthly data sets. The employed temperature data sets are: *Berkeley* [*Rohde et al.*, 2012], *CRUTEM4* (version 4.2), $\mathrm{CRUTEM4_{va}}$ (Variance Adjusted version of CRUTEM4) [*Jones et al.*, 2012], $\mathit{GISTEMP}_{1200}$ (version 2) and $\mathit{GISTEMP}_{250}$ (the suffixes 1200 and 250 indicate the smoothing radius, i.e., the distance in kilometer over which a station influences regional temperature [*Hansen et al.*, 2010]), and *NCDC* (version 3) [*Lawrimore et al.*, 2011]. The employed precipitation data sets are as follows: *CRU* (version 3.21) [*Harris et al.*, 2014], *GPCC* (version 6) [*Schneider et al.*, 2014], *PREC/L* [*Chen et al.*, 2002], *UDEL* (version 3.01) [*Matsuura and Willmott*, 2009], and *VASClimO* (version 1.1) [*Beck et al.*, 2005]. See Tables S1 and S2 in the supporting information for more details. To compare the various data sets, their monthly values are remapped (bilinear interpolation for temperature and conservative remapping for precipitation) from their original resolution to the coarsest grid, defined by CRUTEM4 (5° × 5°).

All the available data are quality checked. To ensure temporal homogeneity, only the pixels with more than 90% of valid data over both subperiods (1981–2010 and 1951–1980) are considered. For precipitation data, we use the GPCC metadata information (i.e., the number of stations contained in each grid box at each month) to define a spatial mask, considering only those grid boxes with at least one station for 90% of the seasons over both subperiods as in *Sun et al.* [2012]. This mask is applied also to the other precipitation data sets considering that, while they have been developed independently, they use similar sets of raw station data. Few grid points

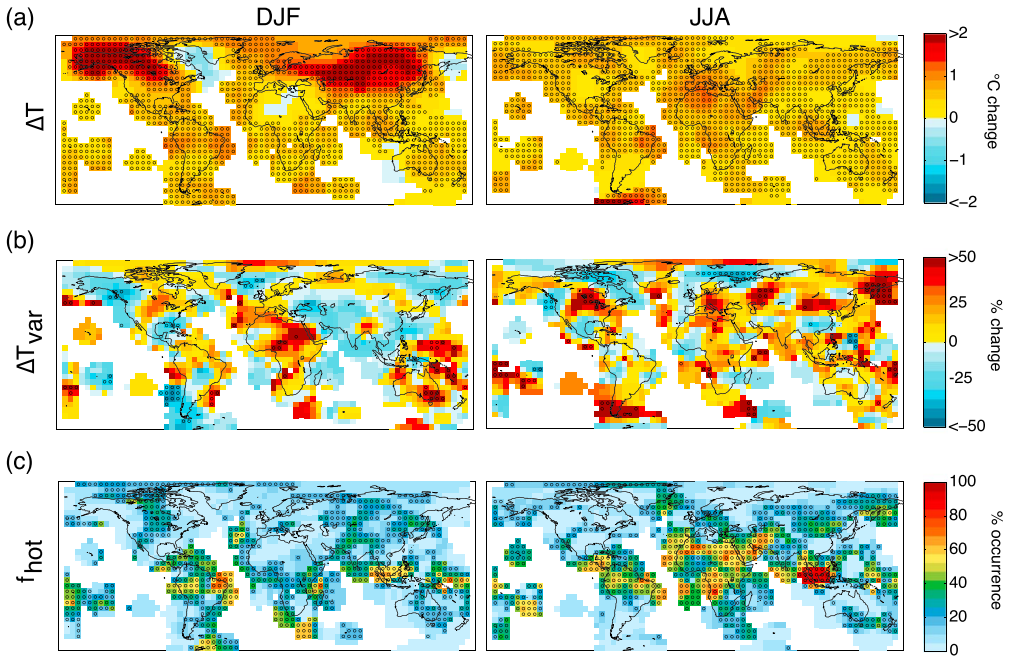

Figure 1. Changes in December-January-February (DJF) and June-July-August (JJA) (a) mean temperature (ΔT), (b) temperature variability (ΔT_{var}), and (c) frequency of seasons with temperatures above the past maximum seasonal temperature (f_{hot}). The changes are calculated between the periods 1981–2010 and 1951–1980 from the GISTEMP$_{1200}$ data set. Black circles indicate significant (at 95% level) changes.

(at most 15 in one data set; see Table S3) show suspicious data leading to anomalous percentual changes (e.g., up to more than 100% in ΔP). This is more likely to happen because there are errors in the data rather than actual changes of such magnitude. As a conservative choice, all available precipitation time series that lead to more than 100% of change for ΔP or ΔP_{var} are excluded from further analysis. Analogously, all available temperature time series that lead to more than 100% of change for ΔT_{var} are excluded.

The results discussed in the main text refer to the GISTEMP$_{1200}$ data set for temperature and to the GPCC data set for precipitation. Taking into account the period 1951–2010 allowed us to consider in the analysis over around 70% of the land surface, thus including highly populated regions but excluding the areas with poor station coverage as the Antarctica, parts of the Arctic (northern Canada, Greenland, Russia), parts of the Amazon, parts of central and northern Africa, and Tibet.

4. Results

Figure 1 shows the observed changes in the three temperature indicators (ΔT, ΔT_{var}, and f_{hot}). The mean temperature indicator (ΔT) shows a clear warming, which is statistically significant in extended areas and for all seasons, with greater changes in central Asia and northern North America, in DJF and MAM (Figures 1a and S1). Similar results are discussed in many other studies [*Hansen et al.*, 2010; *Jones et al.*, 2012; *Muller et al.*, 2013; *Stocker et al.*, 2013].

The temperature variability indicator (ΔT_{var}) displays more heterogeneous values, with large areas of either positive or negative variations (Figures 1b and S2). Currently, there are no robust conclusions about whether temperature variability is changing [*Alexander and Perkins*, 2013], mainly due to data limitations and differences in the methodology for data analysis. The most recent and comprehensive analysis concludes that global temperature variability is not increased while greater changes occurred regionally [*Huntingford et al.*, 2013]. The spatial patterns of temperature variability obtained by *Huntingford et al.* [2013] are consistent with our results. However, contrary to that study, here we also assess the significance of the observed changes and find that such changes are significant only in a few areas of limited extent and for specific seasons. For example, there is a significant increase of DJF temperature variability locally in Africa and Australia, and JJA temperature variability in specific areas in northern North America and Asia (Figure 1b).

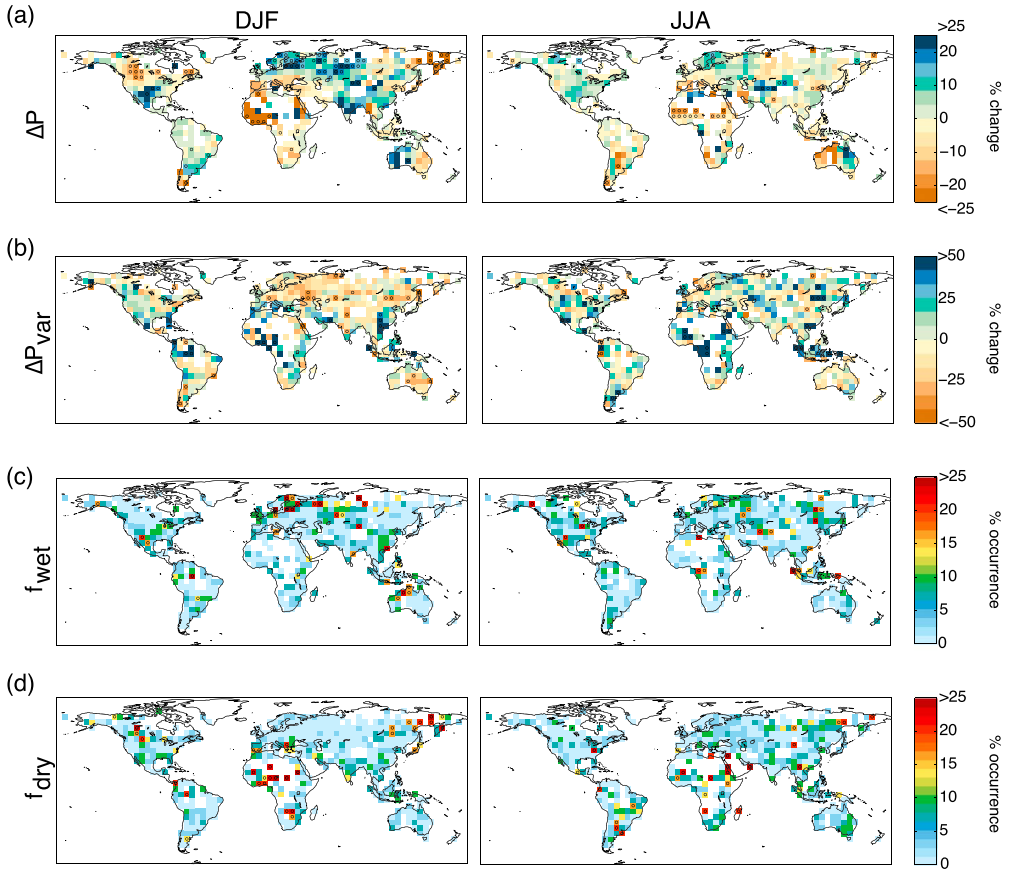

Figure 2. Changes in December-January-February (DJF) and June-July-August (JJA) (a) mean precipitation (ΔP), (b) precipitation variability (ΔP_{var}), (c) frequency of seasons with precipitation above the past maximum seasonal precipitation (f_{wet}), and (d) below the past minimum seasonal precipitation (f_{dry}). The changes are calculated between the periods 1981–2010 and 1951–1980 from the GPCC data set. Black circles indicate significant (at 95% level) changes.

The value of f_{hot} provides complementary information to ΔT and ΔT_{var}. By identifying regions experiencing unprecedented temperatures, for which natural ecosystems and human societies may be unprepared, this indicator helps to highlight areas which are especially vulnerable. The frequency of seasons with temperatures above the past maximum seasonal temperature (f_{hot}) shows large coherent areas with high and significant values (Figures 1c and S3), mostly over low-latitude regions where local warming significantly exceeds the relatively low year-to-year variability. At high latitudes, where both ΔT and the interannual variability are larger, f_{hot} displays lower values. The early emergence of significant warming over low-latitude regions is reported as a robust conclusion in the last IPCC report, and it is supported by both observations [*Diffenbaugh and Scherer*, 2011; *Mahlstein et al.*, 2011] and climate simulations [*Diffenbaugh and Scherer*, 2011; *Mahlstein et al.*, 2011; *Hawkins and Sutton*, 2012; *Diffenbaugh and Giorgi*, 2012].

Changes in precipitation statistics, shown in Figure 2, are generally less pronounced than for temperature and spatially more heterogeneous. Mean precipitation changes (ΔP) reveal a significant decrease of precipitation in central Africa for all seasons and an increase in northern Eurasia, mainly in DJF and MAM (Figures 2a and S4), in agreement with previous studies [*Zhang et al.*, 2007; *Polson et al.*, 2013; *Stocker et al.*, 2013; *Damberg and AghaKouchak*, 2014].

Few localized regions over the globe show significant changes in precipitation variability (ΔP_{var}). These are mainly concentrated in Africa but do not generally exhibit a coherent spatial pattern (Figures 2b and S5). Although the ΔP_{var} indicator has to be considered with caution at local scale, owing to the limited data available, these results suggest that precipitation variability has not changed substantially at global scale, in agreement with *Sun et al.* [2012].

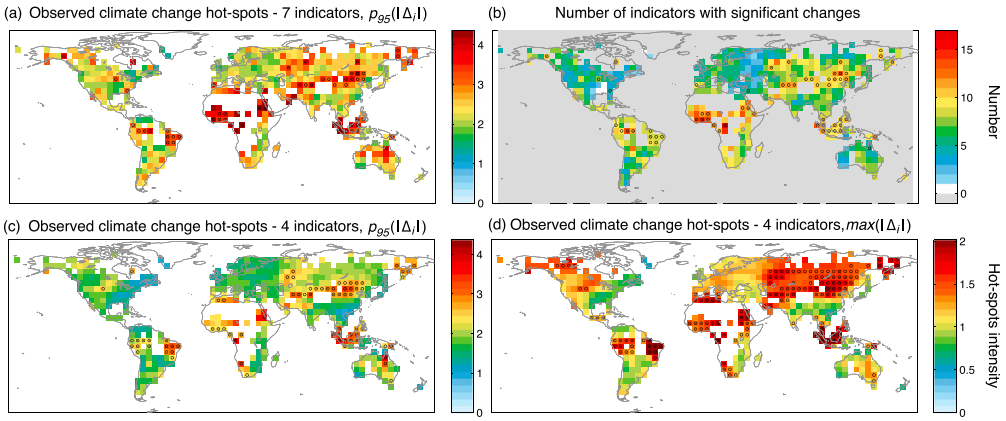

Figure 3. (a) Observed climate change hotspots at grid point scale using the seven indicators and the normalization factor $p_{95}(|\Delta_i|)$; (b) number of individual climate indicators that show significant change; (c) hotspots considering only four indicators (ΔT, ΔT_{var}, f_{hot}, and ΔP) and the normalization factor $p_{95}(|\Delta_i|)$; and (d) the same as Figure 3c but with the normalization factor $\max(|\Delta_i|)$ (the global maximum of the field). The data sets employed are GISTEMP$_{1200}$ and GPCC. Black points (empty circles) indicate significant hotspots at 95% (90%) level.

The frequencies of extremely dry (f_{dry}) and wet (f_{wet}) seasons display rather small changes with respect to past conditions (Figures 2c, 2d, S6, and S7). Areas where such changes are significant generally correspond to locations where the mean precipitation also exhibits significant changes.

We assess the sensitivity of the changes in precipitation and temperature statistics to the choice of specific data sets, repeating our analysis for all observational data sets listed in section 3. Overall, using different observational data sets leads to a similar pattern of changes (Tables S4 and S5). In particular, the agreement is generally high for the temperature statistics and for the precipitation indicators ΔP and ΔP_{var}, while it is lower for f_{dry} and f_{wet}. Interestingly, GISTEMP$_{1200}$ and the *Berkeley* data sets that have similar spatial coverage but are developed following different approaches indicate very similar changes in temperature indicators giving confidence in the results. For precipitation, the analysis is also repeated considering the subperiods 1976–2000 and 1951–1975 and using the data set VASClimo (that provides data till 2000 and is considered a reference for precipitation trend studies, since it is based on a mostly fixed number of stations [*Beck et al.*, 2005; *Wan et al.*, 2013]), obtaining similar results (Table S6).

We proceed and we identify climate change hotspots by condensing the observed temperature and precipitation changes into a single quantity. To this end, we (i) normalize individual climate indicators by the 95th percentile of the distribution of their absolute values and (ii) average the normalized indicators to obtain a single quantity (equation (1)). As done for the individual indicators, we assess the statistical significance of the hotspot index with the same random shuffling Monte Carlo procedure illustrated in section 2.

Figure 3a shows the map of the observed climate change hotspots based on the data sets GISTEMP$_{1200}$ and GPCC. Areas in the central and northern parts of Africa, Indonesia, Amazon, and locally in central eastern Asia are the most prominent observed hotspots. Figure 3b shows the number of climate indicators that exhibit significant changes for each grid box. Two main inferences can be drawn from this figure. First, the hotspots identified here are also those regions with significant changes in the largest number of individual indicators, indicating that the results are substantially robust to variations in the details of the metric used to define the hotspots (as explicitly shown below and in the supporting information). Second, almost the whole spatial domain considered here has experienced significant changes in one or more climate indicators. For this reason, also areas where the change in the hotspot index is small could have had strong changes in a single indicator (e.g., increase in summer temperatures in the Mediterranean region, as shown in Figure 1b).

The hotspot definition is affected by several sources of uncertainty. We first test the sensitivity of our results to the detailed definition of the hotspot index. By removing single indicators, we determine that inclusion/exclusion of ΔP_{var}, f_{dry}, and f_{wet} does not qualitatively change the results (Figure 3c). This result is consistent with the small and nonsignificant changes already detected for these three indicators. Then, in

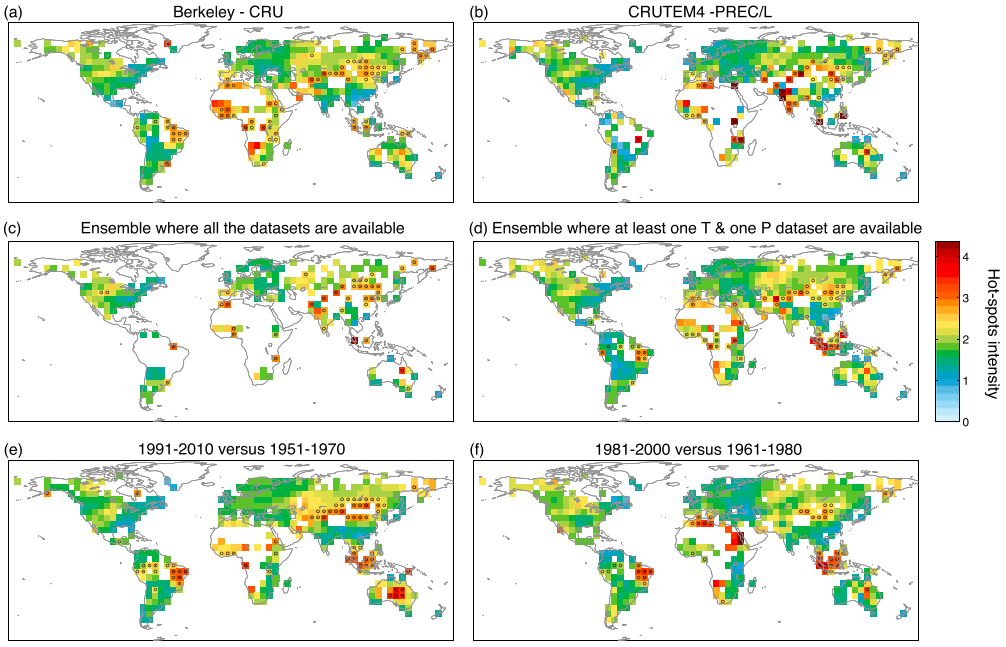

Figure 4. Observed climate change hotspots using different data sets and different subperiods. (a) *Berkeley* and CRU (1951–1980 versus 1981–2010); (b) CRUTEM4 and PREC/L (1951–1980 versus 1981–2010). Using the ensemble of all the available data sets with (c) the hotspots calculated for those grid points where all the data sets are available (1951–1980 versus 1981–2010), or (d) the hotspots calculated for those grid points where at least one temperature and one precipitation data set are available (1951–1980 versus 1981–2010). (e) $GISTEMP_{1200}$ and GPCC (1951–1970 versus 1991–2010); (f) $GISTEMP_{1200}$ and GPCC (1961–1980 versus 1981–2000). The hotspots have been calculated considering the four indicators (ΔT, ΔT_{var}, f_{hot}, and ΔP) and the normalization factor $p_{95}(|\Delta_i|)$. Black points (empty circles) indicate significant hotspots at 95% (90%) level.

addition to the global 95th percentile, which is less affected by outliers, we also consider the 99th percentile and the global maximum value (as in *Diffenbaugh and Giorgi* [2012]). Overall, we found no remarkable changes in the results for the different normalizations (Figures 3d and S8).

The availability and the quality of data remain a key concern, with the caveat that the quality of precipitation data is generally poorer than the quality of temperature data [*Wan et al.*, 2013; *Stocker et al.*, 2013]. We compute the hotspot index with all the 24 possible combinations of pairs of temperature (six data sets) and precipitation data (four data sets for the period 1951–2010). These results are presented in Figures 4a, 4b, and S9. Additionally, we compute the hotspots by incorporating the full ensemble of observed data sets, with an approach similar to that in *Diffenbaugh and Giorgi* [2012] (Figures 4c and 4d; see supporting information for details). Figures 4a–4d and S9 indicate a substantial agreement of the hotspot analyses performed with different databases or with the ensemble of all observations, with some local exceptions. For example, in Figures 4b and 4c, grid points with less significant change are found in the Amazon and in central eastern Asia, but this is mainly due to the fact that not all data sets cover appropriately these areas. Thus, even if the hotspots for individual grid points should be considered with caution, a general consistent pattern emerges from the analysis of the available data, supporting the robustness of the results.

Internal climate variability can play a significant role in multidecadal changes in temperature (as the recent "hiatus" in global warming [*Easterling and Wehner*, 2009; *Steinman et al.*, 2015]) and in precipitation (e.g., the Sahel drought [*Martin and Thorncroft*, 2014]). Previous hotspot analyses based on climate model projections used ensembles of simulations, reducing the influence of multidecadal variability. Our hotspot analysis is based on observations instead, and thus, we are considering an "individual realization," which may be more affected by multidecadal variability. To give some insights into this source of uncertainty, in addition to calculating the hotspots splitting the full 60 year period into two 30 year subperiods, in Figures 4e and 4f we provide two examples of how the hotspots appear if subperiods of 20 years are considered (1991–2010 versus 1951–1970 and 1981–2000 versus 1961–1980). Some local differences arise (e.g., in Australia), with generally

lower hotspot values for the former subperiods (i.e., 1981–2000 versus 1961–1980). However, most significant hotspots persist, mainly because two key indicators of the hotspots, that is, ΔT and f_{hot}, are large enough to mask the natural internal variability.

5. Conclusion

The goal of this letter is to identify the observed climate change hotspots and to analyze the role of the various variables contributing to the hotspot index, that is, the seasonal changes in mean, variability, and extremes of temperature and precipitation. We show that areas in the Amazon, the Sahel, tropical West Africa, Indonesia, and central eastern Asia emerge as primary observed hotspots. A widespread increase in mean temperature, the intensification of extreme hot-season occurrence in low-latitude regions and a precipitation decrease in central Africa, shape the hotspots. Although the hotspots for individual grid points should be considered with caution, we find that the spatial pattern of the hotspots is broadly consistent across variations in the mathematical definition of the hotspot index and observed data sets used. Further, almost the whole analyzed domain has suffered significant changes in one or more hotspot indicators, thus, also the areas not identified as significant hotspots may be vulnerable to climate change.

An expected consequence of the global warming is an increase in climate variability. Drawing on several up-to-date databases representing global monthly mean precipitation and temperature, we found that temperature and precipitation variability have been substantially stable over the past decades at global scale, with few regions showing statistically significant changes. The analysis discussed here is based on monthly data, since they provide a larger global coverage with respect to data aggregated at finer temporal scale. However, monthly mean statistics can underestimate extreme responses. This points to the need for further detailed studies focused on regional (extreme) changes, where suitable data sets are available, possibly adding also information on socio-ecological vulnerability (see, e.g., *Busby et al.* [2014] and *Hagenlocher et al.* [2014] for Africa).

The hotspot definition adopted here follows the model study of *Diffenbaugh and Giorgi* [2012]. They identified areas in the Amazon, the Sahel and tropical West Africa, Indonesia, and the Tibetan Plateau as the most persistent and early emerging prominent hotspots foreseen for the 21st century, under the assumptions of high (RCP8.5) and moderate (RCP4.5) greenhouse gas emission pathways. A notable agreement between observed and projected [*Diffenbaugh and Giorgi*, 2012] climate change hotspots is detected, highlighting that the areas characterized by significant changes in multiple climatic indicators are persistent over time. This suggests that the hotspot regions foreseen for the coming decades have already emerged in current conditions and regional adaptation/impact strategies should have a special focus on such areas. The results discussed here represent important information for decision makers, as they may help to define the most important intervention areas for effective adaptation decisions over near-time horizons.

Acknowledgments

This work is supported by the Italian project of Interest "NextData" of the Italian Ministry for Education, University and Research. We acknowledge the NOAA/OAR/ESRL PSD, Boulder, Colorado, USA, for making the data available on their Web site http://www.esrl.noaa.gov/psd/. All the data sets are provided by the NOAA/OAR/ESRL PSD, except the data set *Berkeley* provided by KNMI Climate Explorer from their website at http://climexp.knmi.nl/.

The Editor thanks two anonymous reviewers for their assistance in evaluating this paper.

References

AghaKouchak, A., L. Cheng, O. Mazdiyasni, and A. Farahmand (2014), Global warming and changes in risk of concurrent climate extremes: Insights from the 2014 California drought, *Geophys. Res. Lett.*, *41*, 8847–8852, doi:10.1002/2014GL062308.

Alexander, L., and S. Perkins (2013), Debate heating up over changes in climate variability, *Environ. Res. Lett.*, *8*(4), 041001.

Baettig, M. B., M. Wild, and D. M. Imboden (2007), A climate change index: Where climate change may be most prominent in the 21st century, *Geophys. Res. Lett.*, *34*, L17711, doi:10.1029/2007GL031628.

Beaumont, L. J., A. Pitman, S. Perkins, N. E. Zimmermann, N. G. Yoccoz, and W. Thuiller (2011), Impacts of climate change on the world's most exceptional ecoregions, *Proc. Natl. Acad. Sci. U.S.A.*, *108*(6), 2306–2311.

Beck, C., J. Grieser, and B. Rudolf (2005), A new monthly precipitation climatology for the global land areas for the period 1951 to 2000. Climate Status Report 2004, *Tech. Rep.*, German Weather Service, Offenbach, Germany.

Busby, J., K. Cook, E. Vizy, T. Smith, and M. Bekalo (2014), Identifying hotspots of security vulnerability associated with climate change in Africa, *Clim. Change*, *124*(4), 717–731.

Bye, J., K. Fraedrich, E. Kirk, S. Schubert, and X. Zhu (2011), Random walk lengths of about 30 years in global climate, *Geophys. Res. Lett.*, *38*, L05806, doi:10.1029/2010GL046333.

Chen, M., P. Xie, J. E. Janowiak, and P. a. Arkin (2002), Global land precipitation: A 50-yr monthly analysis based on gauge observations, *J. Hydrometeorol.*, *3*, 249–266.

Damberg, L., and A. AghaKouchak (2014), Global trends and patterns of drought from space, *Theor. Appl. Climatol.*, *117*, 441–448.

de Sherbinin, A. (2014), Climate change hotspots mapping: What have we learned?, *Clim. Change*, *123*(1), 23–37.

Diffenbaugh, N., and M. Scherer (2011), Observational and model evidence of global emergence of permanent, unprecedented heat in the 20th and 21st centuries, *Clim. Change*, *107*(3–4), 615–624.

Diffenbaugh, N. S., and C. B. Field (2013), Changes in ecologically critical terrestrial climate conditions, *Science*, *341*(6145), 486–492.

Diffenbaugh, N. S., and F. Giorgi (2012), Climate change hotspots in the CMIP5 global climate model ensemble, *Clim. Change*, *114*(3–4), 813–822.

Diffenbaugh, N. S., F. Giorgi, L. Raymond, and X. Bi (2007), Indicators of 21st century socioclimatic exposure, *Proc. Natl. Acad. Sci. U.S.A.*, *104*(51), 20,195–20,198.
Donat, M. G., and L. V. Alexander (2012), The shifting probability distribution of global daytime and night-time temperatures, *Geophys. Res. Lett.*, *39*, L14707, doi:10.1029/2012GL052459.
Donat, M. G., et al. (2013), Updated analyses of temperature and precipitation extreme indices since the beginning of the twentieth century: The HadEX2 dataset, *J. Geophys. Res. Atmos.*, *118*, 2098–118, doi:10.1002/jgrd.50150.
Easterling, D. R., and M. F. Wehner (2009), Is the climate warming or cooling?, *Geophys. Res. Lett.*, *36*, L08706, doi:10.1029/2009GL037810.
Fischer, E. M., and R. Knutti (2014), Detection of spatially aggregated changes in temperature and precipitation extremes, *Geophys. Res. Lett.*, *41*, 547–554, doi:10.1002/2013GL058499.
Giorgi, F. (2006), Climate change hot-spots, *Geophys. Res. Lett.*, *33*, L08707, doi:10.1029/2006GL025734.
Hagenlocher, M., S. Lang, D. Hölbling, D. Tiede, and S. Kienberger (2014), Modeling hotspots of climate change in the Sahel using object-based regionalization of multidimensional gridded datasets, *IEEE J. Sel. Top. Appl. Earth Obs. Remote Sens.*, *7*(1), 229–234.
Hansen, J., M. Sato, J. Glascoe, and R. Ruedy (1998), A common-sense climate index: Is climate changing noticeably?, *Proc. Natl. Acad. Sci.*, *95*(8), 4113–4120.
Hansen, J., R. Ruedy, M. Sato, and K. Lo (2010), Global surface temperature change, *Rev. Geophys.*, *48*, RG4004, doi:10.1029/2010RG000345.
Hansen, J., M. Sato, and R. Ruedy (2012), Perception of climate change, *Proc. Natl. Acad. Sci. U.S.A.*, *109*(37), E2415–E2423.
Hao, Z., A. AghaKouchak, and T. J. Phillips (2013), Changes in concurrent monthly precipitation and temperature extremes, *Environ. Res. Lett.*, *8*(3), 034014.
Harris, I., P. Jones, T. Osborn, and D. Lister (2014), Updated high-resolution grids of monthly climatic observations the CRU TS3.10 dataset, *Int. J. Climatol.*, *34*(3), 623–642.
Hawkins, E., and R. Sutton (2012), Time of emergence of climate signals, *Geophys. Res. Lett.*, *39*, L01702, doi:10.1029/2011GL050087.
Holmgren, M., M. Hirota, E. H. van Nes, and M. Scheffer (2013), Effects of interannual climate variability on tropical tree cover, *Nat. Clim. Change*, *3*(8), 755–758.
Huntingford, C., P. Jones, V. Livina, T. Lenton, and P. Cox (2013), No increase in global temperature variability despite changing regional patterns, *Nature*, *500*(7462), 327–331.
Jones, P. D., D. H. Lister, T. J. Osborn, C. Harpham, M. Salmon, and C. P. Morice (2012), Hemispheric and large-scale land-surface air temperature variations: An extensive revision and an update to 2010, *J. Geophys. Res.*, *117*, D05127, doi:10.1029/2011JD017139.
Karoly, D. J., and K. Braganza (2001), Identifying global climate change using simple indices, *Geophys. Res. Lett.*, *28*(11), 2205–2208.
Kiktev, D., D. M. H. Sexton, L. Alexander, and C. K. Folland (2003), Comparison of modeled and observed trends in indices of daily climate extremes, *J. Clim.*, *16*(22), 3560–3571.
Lawrimore, J. H., M. J. Menne, B. E. Gleason, C. N. Williams, D. B. Wuertz, R. S. Vose, and J. Rennie (2011), An overview of the global historical climatology network monthly mean temperature data set, version 3, *J. Geophys. Res.*, *116*, D19121, doi:10.1029/2011JD016187.
Loarie, S. R., P. B. Duffy, H. Hamilton, G. P. Asner, C. B. Field, and D. D. Ackerly (2009), The velocity of climate change, *Nature*, *462*(7276), 1052–1057.
Mahlstein, I., R. Knutti, S. Solomon, and R. W. Portmann (2011), Early onset of significant local warming in low latitude countries, *Environ. Res. Lett.*, *6*(3), 034009.
Martin, E. R., and C. Thorncroft (2014), Sahel rainfall in multimodel CMIP5 decadal hindcasts, *Geophys. Res. Lett.*, *41*, 2169–2175, doi:10.1002/2014GL059338.
Matsuura, K., and C. J. Willmott (2009), *Terrestrial Precipitation: 1900–2008 Gridded Monthly Time Series (Version 2.01)*, Cen. for Clim. Res., Dep. of Geogr., Univ. of Delaware, Newark, N. J.
Muller, R. A., J. Curry, D. Groom, R. Jacobsen, S. Perlmutter, R. Rohde, A. Rosenfeld, C. Wickham, and J. Wurtele (2013), Decadal variations in the global atmospheric land temperatures, *J. Geophys. Res. Atmos.*, *118*, 5280–5286, doi:10.1002/jgrd.50458.
Piontek, F., et al. (2014), Multisectoral climate impact hotspots in a warming world, *Proc. Natl. Acad. Sci. U.S.A.*, *111*(9), 3233–3238.
Polson, D., G. C. Hegerl, X. Zhang, and T. J. Osborn (2013), Causes of robust seasonal land precipitation changes, *J. Clim.*, *26*(17), 6679–6697.
Rohde, R., R. A. Muller, R. Jacobsen, E. Muller, D. Groom, and C. Wickham (2012), A new estimate of the average Earth surface land temperature spanning 1753 to 2011, *Geoinf. Geostat.*, *1*, 1–7.
Schär, C., P. Vidale, D. Lüthi, and C. Frei (2004), The role of increasing temperature variability in European summer heatwaves, *Nature*, *427*, 3926–3928.
Schneider, U., A. Becker, P. Finger, A. Meyer-Christoffer, M. Ziese, and B. Rudolf (2014), GPCC's new land surface precipitation climatology based on quality-controlled in situ data and its role in quantifying the global water cycle, *Theor. Appl. Climatol.*, *115*(1–2), 15–40.
Steinman, B. A., M. E. Mann, and S. K. Miller (2015), Atlantic and Pacific multidecadal oscillations and Northern Hemisphere temperatures, *Science*, *347*(6225), 988–991.
Stocker, T. F., D. Qin, G.-K. Plattner, M. Tignor, S. Allen, J. Boschung, A. Nauels, Y. Xia, V. Bex, and P. Midgley (Eds.) (2013), *Climate Change 2013: The Physical Science Basis. Contribution of Working Group I to the Fifth Assessment Report of the Intergovernmental Panel on Climate Change*, Cambridge Univ. Press, Cambridge, U. K., and New York.
Sun, F., M. L. Roderick, and G. D. Farquhar (2012), Changes in the variability of global land precipitation, *Geophys. Res. Lett.*, *39*, L19402, doi:10.1029/2012GL053369.
Tsonis, A. A. (1996), Widespread increases in low-frequency variability of precipitation over the past century, *Nature*, *382*(6593), 700–702.
Wan, H., X. Zhang, F. W. Zwiers, and H. Shiogama (2013), Effect of data coverage on the estimation of mean and variability of precipitation at global and regional scales, *J. Geophys. Res. Atmos.*, *118*, 534–546, doi:10.1002/jgrd.50118.
Williams, J. W., S. T. Jackson, and J. E. Kutzbach (2007), Projected distributions of novel and disappearing climates by 2100 AD, *Proc. Natl. Acad. Sci. U.S.A.*, *104*(14), 5738–5742.
Zhang, X., F. W. Zwiers, G. C. Hegerl, F. H. Lambert, N. P. Gillett, S. Solomon, P. A. Stott, and T. Nozawa (2007), Detection of human influence on twentieth-century precipitation trends, *Nature*, *448*(7152), 461–466.